Received: 18 September 2018 | Revised: 25 February 2019 | Accepted: 6 March 2019

DOI: 10.1111/ijpo.12531

ORIGINAL RESEARCH

WILEY pediatricobesity

Brown adipose tissue estimated with the magnetic resonance imaging fat fraction is associated with glucose metabolism in adolescents

Elin Lundström[1] | Joy Ljungberg[1] | Jonathan Andersson[1] | Hannes Manell[2,3,4] | Robin Strand[1,5] | Anders Forslund[2,3] | Peter Bergsten[2,3,4] | Daniel Weghuber[6,7] | Katharina Mörwald[6,7] | Fanni Zsoldos[6,7] | Kurt Widhalm[6,7,8] | Matthias Meissnitzer[9] | Håkan Ahlström[1,10] | Joel Kullberg[1,10]

[1] Department of Surgical Sciences, Section of Radiology, Uppsala University, Uppsala, Sweden

[2] Department of Women's and Children's Health, Uppsala University, Uppsala, Sweden

[3] Children Obesity Clinic, Uppsala University Hospital, Uppsala, Sweden

[4] Department of Medical Cell Biology, Uppsala University, Uppsala, Sweden

[5] Department of Information Technology, Uppsala University, Uppsala, Sweden

[6] Department of Pediatrics, Paracelsus Medical University, Salzburg, Austria

[7] Obesity Research Unit, Paracelsus Medical University, Salzburg, Austria

[8] Department of Pediatrics, Medical University of Vienna, Vienna, Austria

[9] Department of Radiology, Paracelsus Medical University, Salzburg, Austria

[10] Antaros Medical, BioVenture Hub, Mölndal, Sweden

Correspondence
Elin Lundström, Department of Surgical Sciences, Section of Radiology, MRT, Entrance 24, Uppsala University Hospital, SE-751 85 Uppsala, Sweden.
Email: elin.lundstrom@radiol.uu.se

Funding information
Regional Research Council in Uppsala, Grant/Award Numbers: 233041 and 309901; Swedish Heart-Lung Foundation, Grant/Award Number: 2170492; Swedish Research Council,

Summary

Background: Despite therapeutic potential against obesity and diabetes, the associations of brown adipose tissue (BAT) with glucose metabolism in young humans are relatively unexplored.

Objectives: To investigate possible associations between magnetic resonance imaging (MRI) estimates of BAT and glucose metabolism, whilst considering sex, age, and adiposity, in adolescents with normal and overweight/obese phenotypes.

Methods: In 143 subjects (10-20 years), MRI estimates of BAT were assessed as cervical-supraclavicular adipose tissue (sBAT) fat fraction (FF) and T_2^* from water-fat MRI. FF and T_2^* of neighbouring subcutaneous adipose tissue (SAT) were also assessed. Adiposity was estimated with a standardized body mass index, the waist-to-height ratio, and abdominal visceral and subcutaneous adipose tissue volumes. Glucose metabolism was represented by the 2h plasma glucose concentration, the Matsuda index, the homeostatic model assessment of insulin resistance, and the oral disposition index; obtained from oral glucose tolerance tests.

Results: sBAT FF and T_2^* correlated positively with adiposity before and after adjustment for sex and age. sBAT FF, but not T_2^*, correlated with 2h glucose and Matsuda index, also after adjustment for sex, age, and adiposity. The association with 2h glucose persisted after additional adjustment for SAT FF.

Conclusions: The association between sBAT FF and 2h glucose, observed independently of sex, age, adiposity, and SAT FF, indicates a role for BAT in glucose metabolism, which potentially could influence the risk of developing diabetes. The lacking

Elin Lundström and Joy Ljungberg contributed equally to this work.

Grant/Award Number: 2016-01040; European Union's Seventh Framework Programme (FP7/2007-2013), Grant/Award Number: 279153

association with sBAT T_2^* might be due to FF being a superior biomarker for BAT and/or to methodological limitations in the T_2^* quantification.

KEYWORDS

adolescent, brown adipose tissue, glucose metabolism, magnetic resonance imaging

1 | INTRODUCTION

The human brown adipose tissue (BAT) has a therapeutic potential against obesity and related diabetes owing to its ability to dissipate energy through nonshivering thermogenesis (NST) when activated, eg, in response to cold exposure.[1-3] After infancy, the major BAT depot is located in the cervical-supraclavicular region.[1,4] Based on observations in adults, this depot likely contains brown adipocytes of both classic brown and recruitable beige origin,[5-7] intermixed with white adipose tissue (WAT) composed of white adipocytes.[8,9] Potential therapies aiming at increasing the amount and/or thermogenic capacity of the two types of brown adipocytes have been discussed.[3,10] Despite the therapeutic potential, the knowledge of possible associations between BAT and glucose metabolism in humans is still relatively limited.

In vivo studies in adults, using positron emission tomography (PET) combined with computed tomography (CT) to assess BAT activity from [^{18}F]fluorodeoxyglucose (FDG) uptake, have shown negative relationships both between BAT activity and adiposity[11,12] and between prevalence of BAT activity and age.[13,14] Positive relationships between adiposity and age have also been observed, but only in subjects with no visualized cold-induced BAT activity.[14] These results indicate a potential role for BAT in prevention of long-term fat accumulation, which could lead to overweight and obesity during adulthood. Relatively large cohort studies of mainly adult patients (n = 1972[13] and n = 3614[15]) showed higher prevalence of active BAT in females compared with males. However, smaller studies performed with cold exposure (n = 10[16] and n = 17[17]) reported no observable BAT-related differences between the sexes. These discrepancies could be because of either differences in statistical power or to the generally colder temperatures required for inducing NST in males than in females.[18] Corresponding associations have also been studied in pediatric patients where a negative correlation between BAT activity and adiposity and an age-dependence in BAT activity, which peaked at 13 to 15 years, have been observed.[4] However, no clear adiposity-related[19] or sex-related[4,19] differences in BAT prevalence have been observed at the ambient temperatures used for clinical examinations. Because of differences in body composition and metabolism between adults and children, the relationships observed in adults might not be directly transferable to children. This together with the knowledge of child obesity being a risk factor for adult obesity[20] strongly suggest dedicated BAT studies in children and adolescents.

Magnetic resonance imaging (MRI) has been introduced as a nonionizing imaging alternative and complement to FDG-PET/CT. Quantitative fat fraction (FF) and T_2^* maps can be estimated from water-fat MRI. FF is calculated as the fraction of the fat signal to the total signal of water and fat.[21] T_2^* refers to the joint effective transverse relaxation time for the water and fat signals.[21] In adipose tissue depots, the presence of BAT is indicated by a relatively low FF and T_2^* compared with in more pure WAT, such as subcutaneous adipose tissue (SAT).[22-24] The comparably low FF of BAT is likely due to a lower concentration of intracellular lipids, a higher concentration of intracellular water, and richer vascularization. The relatively low T_2^* of BAT may be due to its abundance of blood vessels and iron-rich mitochondria, possibly in combination with a different blood oxygenation level from that of WAT. These properties may cause local inhomogeneities of the static magnetic field, generated by the MR system, which in turn might influence the tissue T_2^*. Studies using cold-induced FDG uptake to confirm the presence of functional BAT indicate FF and T_2^* as suitable MRI estimates of BAT regardless of its activation status (ie, both during warm and cold conditions).[23,24] Hitherto, there is no available imaging method for quantifying BAT amount in terms of, eg, mass of brown adipocytes.[25] However, BAT activity estimated during cold exposure has shown inverse relationships to FF[24,26] and T_2^*[24] estimated during warm conditions. In this study, we therefore assumed the two MRI estimates of BAT, assessed in room temperature, to be inversely related to BAT amount in terms of the concentration of brown adipocytes. A study in children has shown lower FF and T_2^* in the supraclavicular depot compared with the subcutaneous depot.[27] This is in accordance with a higher BAT content in the supraclavicular depot. Moreover, the supraclavicular FF and T_2^* have been observed to be positively associated with adiposity in children,[27,28] whereas no relationship with age has been observed.[27]

By studying the associations between BAT and adiposity-related glucose metabolism, the possible involvement of this tissue in the development of diabetes could be elucidated. Human BAT is an insulin-sensitive tissue with a glucose uptake rate similar to that of skeletal muscle under insulin stimulation.[29] Studies in adults have shown relationships between supraclavicular FF and insulin sensitivity[26,30] and also an improved insulin sensitivity from cold exposure aiming for BAT activation or recruitment.[31,32] Despite research efforts in adult humans, in vivo imaging studies targeting the role of BAT in glucose metabolism in children and adolescents are still limited.

The purpose of this work was to investigate possible associations of FF and T_2^* of cervical-supraclavicular adipose tissue (ie, suspected BAT, here denoted *sBAT*) with glucose metabolism, whilst considering sex, age, and adiposity, in adolescents with normal and overweight/obese phenotypes.

2 | METHODS

2.1 | Subjects

This study was conducted using data from the European cohort study, *Beta-cell function in Juvenile Diabetes and Obesity* (Beta-JUDO, FP7-HEALTH-2011-two-stage, project number: 279153), where children and adolescents were recruited and examined at two research sites: Uppsala, Sweden, and Salzburg, Austria. The study had obtained ethical approval from the Regional Ethical Review Boards in both cities. Informed written consent was obtained from the subjects and their guardians. The study was conducted throughout the year. In Uppsala, subjects with overweight or obesity were recruited from an obesity specialist clinic to which they had been referred from the primary health care after inadequate treatment results. In Salzburg, patients that were overweight or had obesity were recruited at a similar specialist clinic with or without prior referral from primary health care. Children and adolescents with normal weight were recruited as controls from schools in Uppsala. Only individuals imaged with MRI (n = 162) were considered for inclusion in this study. Of these, 18 individuals were excluded due to poor image quality (primarily because of severe motion artefacts) and one individual was excluded due to the segmented sBAT volume being too small for reliable FF and T_2^* measurements. Eight subjects showed insufficient sBAT segmentations during visual review but remained included after manual removal of obvious non-sBAT structures (eg, SAT). Twenty-one subjects showed insufficient segmentations of neighbouring SAT from the back (bSAT). These segmentations were also manually corrected. One patient was excluded from the glucose metabolism analyses because of being an outlier as a result of diagnosed diabetes. The age span of included subjects was 10 to 20 years. The majority consisted of patients (n = 126) and the remaining part of controls (n = 17). For statistical comparisons, the subjects were divided into three groups according to the recruitment and examination procedures: Salzburg patients, Uppsala patients, and controls. Within the three groups, the majority of subjects were Caucasian (65/82 Salzburg patients, 38/44 Uppsala patients, and 15/17 controls) and a minority were of other origin (11/82 Salzburg patients, 6/44 Uppsala patients, and 2/17 controls). The remaining 6/82 Salzburg patients had lacking ethnicity data.

2.2 | Height, weight, and adiposity measurements

Height and weight of the subjects were obtained using calibrated scales (Seca, Hamburg, Germany) and stadiometers (Uppsala: Ulmer [Busse Design + Engineering GmbH, Elchingen, Germany]; Salzburg: Seca). Waist circumference was obtained using flexible tape, midway between the lowest rib and the superior border of the iliac crest, on a standing subject. Measurements of adiposity were represented by the waist-to-height ratio ($WHtR = waist/height$), standardized body mass index (sBMI), and volumetric measurements of the abdominal subcutaneous and visceral adipose tissues (aSATvol and aVATvol, respectively). The age- and gender-adjusted BMI (ie, the sBMI) was calculated according to the World Health Organization 2006 to 2007 growth reference (http://www.who.int/growthref/en/). aSATvol and aVATvol were obtained from the MRI data (see subsection 2.5).

2.3 | Glucose metabolism measurements

To evaluate glucose metabolism, each subject underwent an oral glucose tolerance test (OGTT), from which measurements of plasma glucose and insulin levels were obtained. The OGTT was performed according to a previously described procedure.[33] Additional information on handling and analyses of the blood samples is provided in the Data S1. Four relevant parameters, reflecting different aspects of glucose metabolism during fasting and during a glucose challenge, were calculated from the OGTT. The parameters were the concentration of plasma glucose at 120 minutes (2h glucose), the Matsuda index, the homeostatic model assessment of insulin resistance (HOMA-IR), and the oral disposition index (DI_O). 2h glucose is inversely related to glucose tolerance. Subjects with 7.8 mmol/l $\leq$ 2h glucose < 11.1 mmol/l were considered to have prediabetes and subjects with 2h glucose $\geq$ 11.1 mmol/l were considered to have diabetes.[34] Matsuda index is an estimate of whole-body insulin sensitivity and was calculated from the plasma glucose and insulin concentrations at five time points during the OGTT[35] (according to http://mmatsuda.diabetes-smc.jp/english.html). HOMA-IR indicates insulin resistance and was obtained from the baseline (fasting) values of the plasma glucose and insulin levels.[36] The DI_O provides a proxy measurement of beta cell function, adjusted for insulin sensitivity, and was obtained from the fasting insulin concentration and the change in plasma glucose and insulin concentrations during the first 30 minutes of the OGTT.[37] Fasting levels were obtained from samples collected 5 minutes prior to the start of the test. Unit conversion factors (glucose concentration: from [mmol/l] to [mg/dl]; insulin concentration: from [pmol/l] to [μU/ml]) were obtained from http://mmatsuda.diabetes-smc.jp/english.html.

2.4 | Puberty

Puberty was evaluated with Tanner staging[38,39] and subcategorized according to prepuberty (Tanner 1), puberty (Tanner 2-4), and postpuberty (Tanner 5). For subjects lacking Tanner staging, biochemical parameters and growth spurt were used as substituting estimates. Additional information on the biochemical parameters is provided in Data S1. In this study, puberty was only included in the evaluations to determine whether it had a considerable impact on the associations as compared with age.

2.5 | Magnetic resonance imaging

At both sites, MRI was performed on clinical whole-body 1.5 T MR systems (Uppsala: Philips Achieva; Salzburg: Philips Ingenia, both Philips Healthcare, Best, The Netherlands). Imaging was carried out at room temperature, without prior cold or warm preparation of the subjects, after a standardized light meal and preferably on the same

TABLE 1 Summary of imaging details for the water-fat data

Imaging Parameter	sBAT Sequence	Abdominal Sequence
Pulse sequence	3D multi-echo gradient echo	3D multi-echo gradient echo
Coil	Neurovascular (Uppsala), dS Base + dS Head + FlexCoverage anterior and posterior (Salzburg)	Built-in body coil
Scan volume localization	Cervical-supraclavicular fat depot	Centred at lumbar vertebrae 3 to 4
Gating/triggering	Shallow breathing	Breath-hold
Orientation	Axial	Axial
Repetition time	32.7 ms	8.8 ms
Echo time 1/Echo time spacing	1.68/2.87 ms (Uppsala), 1.59/2.93 ms (Salzburg)	1.38/2.60 ms
Number of echoes	6 (unipolar)	3 (unipolar)
Flip angle	6°	5°
Field of view (RL × AP × FH)	480 × 200 × 50 mm^3	530 × 375 × 168 mm^3
Acquired/reconstructed voxel size (RL × AP × FH)	1.0 × 1.0 × 2/1.0 × 1.0 × 2 mm^3	2.76 × 3.95 × 8/2.07 × 2.07 × 8 mm^3
Number of slices	25	21
Scan duration	4 min and 40 s	17 s

Note. The flip angle was chosen small to reduce T_1-weighting. No contrast agents or pharmacological agents were administered.

Abbreviations: 3D, three-dimensional; AP, anterior-posterior; FH, feet-head; RL, right-left; sBAT, cervical-supraclavicular adipose tissue.

day as the OGTT. The MRI estimates of BAT were represented by sBAT FF and T_2^*, obtained from water-fat MRI (imaging details presented in Table 1). The same image data were also used for estimating bSAT FF and T_2^*. The volumetric abdominal adiposity measurements, aSATvol and aVATvol, were obtained from water-fat MRI of a separate image volume (length 168 mm along the feet-head direction and centred between the lumbar vertebrae 3 and 4, further imaging details presented in Table 1). Previously described methods were used for water-fat reconstruction of sBAT[21] and abdominal[40] image data. Mean sBAT FF and T_2^* were estimated from segmentations obtained by a modified version of a previously presented automated method[41] (see examples of segmentations in Figure 1). Automated segmentations of posteriorly located SAT were performed by isolating adipose tissue between the dorsal muscles and the skin using in-house software. Fine adjustments of the bSAT segmentations were carried out using the same erosion steps and threshold levels for FF and T_2^* as were used for the sBAT segmentations. The aSATvol and aVATvol were segmented according to the following steps: (a) Background was removed using a manually set threshold for the voxel intensities. (b) Foreground voxels with FF $\geq$ 50% were considered as adipose tissue. (c) aSATvol was automatically separated by in-house software using a previously described filtering technique.[42] (d) From the residual adipose tissue, fat surrounding the vertebrae was automatically removed and the remaining part was considered as aVATvol. The MRI data from both research sites were reconstructed and post-processed centrally.

2.6 | Statistics

This work was carried out as an exploratory substudy of Beta-JUDO, where all available data were considered and no power analysis was performed. The analyses comprised all subjects for which the relevant data were available. Subject group comparisons were conducted for a data overview and for investigating possible site-specific differences, ie, those related to examination procedures, prior to performing regression analysis. For normally distributed data (weight, height, waist, sBMI, WHtR, aSATvol, 2h glucose, sBAT FF, and sBAT T_2^*), the possible differences between group means were evaluated using two-tailed Student's *t* test, corrected for differences in variance using Welch's correction. For non-normally distributed data (age, aVATvol, Matsuda index, HOMA-IR, DI_O, bSAT FF, and bSAT T_2^*), possible group differences were tested using Mann-Whitney U test. Fisher's exact test was used to test for differences in the fractions of females and males between the groups. Wilcoxon signed rank test was applied to investigate differences in FF and T_2^* between sBAT and bSAT.

The associations between the MRI estimates of BAT and age and adiposity and glucose metabolism were analyzed using simple linear regression. Instead of HOMA-IR, the logarithm of HOMA-IR (log_{10}HOMA-IR) was employed to attain an approximate linear relationship to sBAT FF. After simple linear regression analyses, each model was adjusted for a set of potential confounding factors: sex, age (basic confounders), and site of examination (methodological confounder), using multiple linear regression analyses. The models that included glucose metabolism parameters were additionally adjusted for sBMI (whole-body adiposity), and aSATvol and aVATvol (local distribution of adiposity). Thus, the multiple linear regressions that included glucose metabolism parameters were carried out using two different sets of potential confounding factors: (a) sex, age, site of examination, and sBMI; (b) sex, age, site of examination, aSATvol, and aVATvol.

In this work, Beta refers to the unstandardized regression coefficient. *P* values < .05 were considered as statistically significant and no correction for multiple testing was applied. All statistical analyses

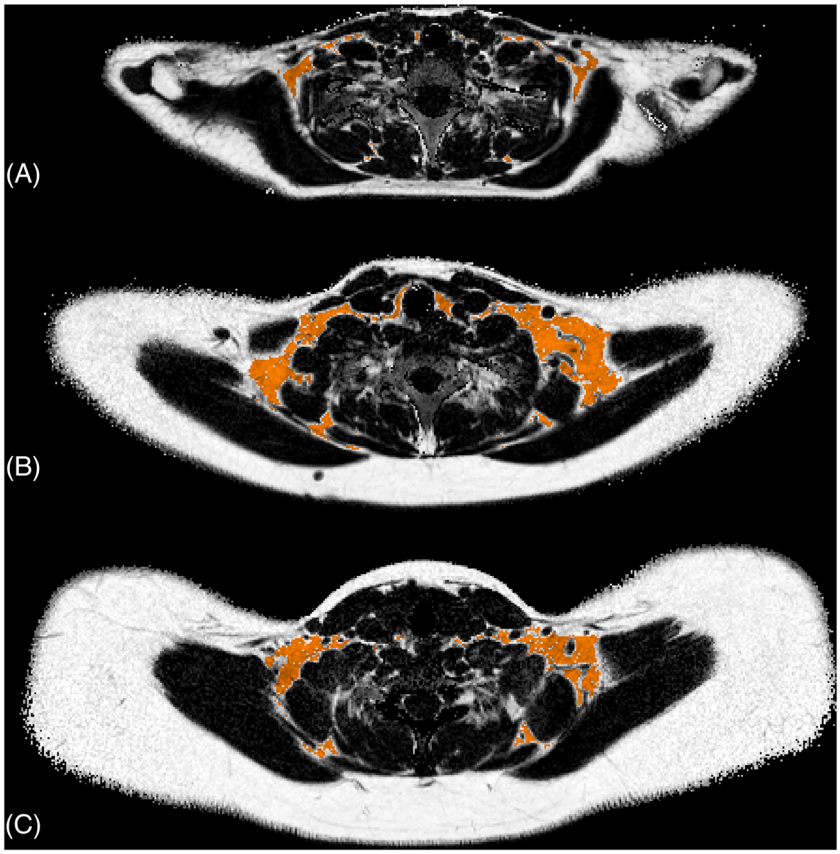

FIGURE 1 Examples of cervical-supraclavicular adipose tissue depot (sBAT) segmentations in three subjects with different amounts of adiposity, defined according to the standardized body mass index (sBMI): Subject A, sBMI = 20.6 kg/m^2, age = 14.6 years; Subject B, sBMI = 30.6 kg/m^2, age = 15.1 years; and Subject C, sBMI = 45.5 kg/m^2, age = 17.9 years. The sBAT segmentations (orange) are overlaid with the corresponding axial fat fraction (FF) maps from which noise in the background (air and cortical bone) has been removed

were performed using Statistica 13.2 to 13.4 (StatSoft Scandinavia AB, Uppsala, Sweden) for Windows. Additional statistics information is provided in Data S1.

3 | RESULTS

Descriptive statistics and group comparisons of basic characteristics, adiposity parameters, glucose metabolism parameters, sBAT FF and T_2^*, and bSAT FF and T_2^* are summarized in Table 2. The associations of sBAT FF and T_2^* with age and adiposity, as obtained by linear regression, are presented in Table 3. The corresponding associations of sBAT FF and T_2^* with glucose metabolism parameters are presented in Table 4 .

3.1 | Group differences

As seen in Table 2, all three groups contained both male and female subjects with the proportion of males ranging from 35 to 52%, but with no significant bias in sex distribution. The controls had lower weights and smaller waist circumferences compared with the patients. There was no significant difference between the three groups in either age or height. All adiposity measurements were lower for controls than for patients. Of the two patient groups, the Uppsala patients showed the overall highest adiposity. Compared with the patients, the controls had higher insulin sensitivity (Matsuda index) and beta cell function (DI_O) and lower insulin resistance (HOMA-IR) and 2h glucose (however, no significant difference was observed between controls and Salzburg patients in 2h glucose). In addition, the Salzburg patients had lower 2h glucose and insulin resistance than the Uppsala patients, but there was no statistically significant difference in insulin sensitivity and beta cell function between the two patient groups. Within the three groups, prediabetes was observed in 28 subjects (four Salzburg patients, 22 Uppsala patients, and two Uppsala controls), and one subject was diagnosed with diabetes (Uppsala patient). FF and T_2^* of both sBAT and bSAT differed between the three groups, with Uppsala patients showing the highest values and Uppsala controls showing the lowest values for both metrics. From group comparisons of all subjects, both FF and T_2^* were observed to be significantly lower in sBAT compared with bSAT ($P < .001$ for both cases, data not presented).

3.2 | Associations

3.2.1 | Sex, age, and puberty

The group comparisons showed no significant difference in sBAT FF or T_2^* between males and females (mean FF difference = 0.96 percentage points (pp), $p = .297$, mean T_2^* difference = 0.66 ms, $p = .471$, data not presented). As seen in Table 3, sBAT FF and T_2^* showed significant but very weak positive linear correlations with age, both before and after adjustment for sex and site. As seen in Table 4, the significance of the association between sBAT FF and age became dependent on the additional explanatory variables used, whereas the association between sBAT T_2^* and age remained significant in all cases. When

TABLE 2 Summary of descriptive statistics and group comparisons of the study population

	Subjects				*P* Value		
	All (n = 143)	PS (n = 82)	PU (n = 44)	C (n = 17)	PS vs PU	PS vs C	PU vs C
Basic characteristics							
Male (n)	71	43	22	6	.853[a]	.287[a]	.394[a]
Female (n)	72	39	22	11			
Age (years)	14.28 ± 2.23	14.10 ± 2.25	14.65 ± 2.31	14.19 ± 1.91	.156[b]	.791[b]	.381[b]
Weight (kg)	87.86 ± 23.88	90.00 ± 21.64	96.52 ± 20.74	55.13 ± 12.90	.101	<.001	<.001
Height (cm)	166.46 ± 10.37	166.07 ± 10.18	167.23 ± 10.59	166.33 ± 11.23	.553	.931	.777
Waist (cm)	101.37 ± 17.07 (n = 140)	103.87 ± 13.50	109.26 ± 11.54 (n = 41)	70.30 ± 7.70	.024	<.001	<.001
Adiposity							
sBMI ($kg \cdot m^{-2}$)	33.63 ± 5.74	34.84 ± 4.22	35.91 ± 3.11	21.87 ± 2.69	.107	<.001	<.001
WHtR	0.61 ± 0.09 (n = 140)	0.63 ± 0.07	0.65 ± 0.05 (n = 41)	0.42 ± 0.03	.014	<.001	<.001
aVATvol (l)	1.45 ± 0.70 (n = 142)	1.46 ± 0.58	1.81 ± 0.63	0.40 ± 0.24 (n = 16)	.001[b]	<.001[b]	<.001[b]
aSATvol (l)	6.29 ± 2.66 (n = 142)	6.71 ± 2.16	7.33 ± 1.86	1.28 ± 0.84 (n = 16)	.098	<.001	<.001
Glucose metabolism							
2h glucose	6.48 ± 1.51 (n = 137)	5.90 ± 1.17 (n = 81)	7.83 ± 1.33 (n = 40)	6.09 ± 1.34 (n = 16)	<.001	.599	<.001
Matsuda index	3.77 ± 3.06 (n = 122)	3.38 ± 2.02 (n = 72)	2.70 ± 1.64 (n = 34)	7.81 ± 5.45 (n = 16)	.080[b]	<.001[b]	<.001[b]
HOMA-IR	3.50 ± 2.34 (n = 130)	3.33 ± 1.83 (n = 76)	4.75 ± 2.97 (n = 37)	1.52 ± 0.81	.008[b]	<.001[b]	<.001[b]
DI_O	3.29 ± 2.55 (n = 127)	3.29 ± 2.74 (n = 75)	2.49 ± 1.72 (n = 35)	4.94 ± 2.42	.149[b]	<.001[b]	<.001[b]
MRI							
sBAT FF (%)	84.87 ± 5.51	84.67 ± 4.39	88.44 ± 3.51	76.62 ± 5.62	<.001	<.001	<.001
sBAT T_2^* (ms)	49.37 ± 5.45	48.73 ± 4.75	52.42 ± 5.31	44.61 ± 4.67	<.001	.003	<.001
bSAT FF (%)	92.78 ± 4.20	93.53 ± 1.53	95.05 ± 0.99	83.29 ± 5.38	<.001[b]	<.001[b]	<.001[b]
bSAT T_2^* (ms)	54.08 ± 4.64	53.89 ± 3.70	56.44 ± 3.12	48.91 ± 7.16	<.001[b]	.003[b]	<.001[b]

Note. Measurements reported as group means ± standard deviations (n = number of subjects in each group or number of measurements, in case measurements were lacking for some subjects in the group). Units of glucose metabolism parameters: 2h glucose ($mmol \cdot l^{-1}$), Matsuda index ($dl \cdot mg^{-1} \cdot ml \cdot \mu U^{-1}$), HOMA-IR ($mmol \cdot l^{-1} \cdot \mu U \cdot ml^{-1}$), and DI_O ($l \cdot mmol^{-1}$). *P* values refer to group comparisons between the patients in Salzburg and Uppsala (PS vs PU), between patients in Salzburg and controls (PS vs C) and between patients in Uppsala and controls (PU vs C).

Abbreviations: aSATvol, volume of abdominal subcutaneous adipose tissue; aVATvol, volume of abdominal visceral adipose tissue; bSAT, subcutaneous adipose tissue of the back; C, Controls Uppsala; DI_O, oral disposition index; FF, fat fraction; HOMA-IR, homeostatic model assessment of insulin resistance; MRI, magnetic resonance imaging; PS, Patients Salzburg; PU, Patients Uppsala; sBAT, cervical-supraclavicular adipose tissue; sBMI, standardized body mass index; WHtR, waist-to-height ratio.

[a]*P* value from Fisher's exact test.

[b]*P* value from Mann-Whitney U test. Remaining *P* values are from Student's *t* test.

investigating the association of sBAT FF and T_2^* with pubertal status (using the set of confounding factors: sex, age, site, and sBMI), the previously significant associations with age remained significant. However, pubertal status did not emerge as a significant explanatory variable (data not presented).

3.2.2 | Adiposity

In the simple linear regressions (Table 3), both sBAT FF and T_2^* correlated significantly with each one of the adiposity measurements of which aVATvol was the best explanatory variable overall. The adiposity measurements also correlated strongly with each other (range: R^2 = .77-.87, *P* < .001, data not presented), with the exception of aVATvol for which the association with the other measurements was weaker (range: R^2 = .45-.46, *P* < .001, data not presented). In the multiple linear regressions (Table 3), the correlations of sBAT FF and T_2^* with the adiposity measurements remained significant also after adjustment for sex, age, and site, still with aVATvol as the best explanatory variable.

3.2.3 | Glucose metabolism

In the simple linear regressions (Table 4), sBAT FF and T_2^* correlated very weakly to moderately with 2h glucose, Matsuda index, and HOMA-IR (or log_{10}HOMA-IR). In addition, sBAT FF but not T_2^* correlated very weakly with DI_O. The associations with 2h glucose and

TABLE 3 Associations of sBAT FF and T_2^* with age and adiposity (main explanatory variables) obtained using simple linear regression and after adjustment for multiple factors using multiple linear regression

	Simple Linear Regression				Multiple Linear Regression				
Variables	**Beta**	**95% CI**	**R^2**	***P* value**	**Beta**	**95% CI**	**R^2**	***P* values**	
sBAT FF vs								**Main**	**Sex/Age/Site**
Age (years)	0.49	0.09 to 0.89	.03	.018	0.47	0.07 to 0.88	.03	.023	.337/NA/.724
sBMI ($kg{\cdot}m^{-2}$)	0.62	0.50 to 0.74	.41	<.001	0.66	0.54 to 0.78	.47	<.001	.838/.014/.002
WHtR	41.56	34.45 to 48.66	.49	<.001	42.76	35.57 to 49.95	.52	<.001	.621/.153/.007
aVATvol (l)	5.41	4.50 to 6.33	.49	<.001	6.26	5.25 to 7.27	.53	<.001	.001/.091/.171
aSATvol (l)	1.32	1.07 to 1.58	.43	<.001	1.42	1.16 to 1.69	.46	<.001	.341/.470/.001
aVATvol (l) and aSATvol (l)					4.30 and 0.70	2.99 to 5.61 and 0.38 to 1.02	.58	<.001 and <.001	.048/.032/.011
sBAT T_2^* vs								**Main**	**Sex/Age/Site**
Age (years)	0.98	0.61 to 1.35	.16	<.001	0.95	0.58 to 1.33	.16	<.001	.535/NA/.180
sBMI ($kg{\cdot}m^{-2}$)	0.39	0.25 to 0.54	.16	<.001	0.43	0.30 to 0.56	.35	<.001	.959/<.001/.003
WHtR	25.56	16.71 to 34.42	.19	<.001	25.33	16.91 to 33.76	.32	<.001	.899/<.001/.010
aVATvol (l)	4.14	3.04 to 5.24	.28	<.001	3.92	2.72 to 5.12	.35	<.001	.083/.006/.052
aSATvol (l)	0.95	0.65 to 1.25	.21	<.001	0.88	0.58 to 1.18	.32	<.001	.611/.001/.004
aVATvol (l) and aSATvol (l)					2.74 and 0.42	1.11 to 4.37 and 0.02 to 0.82	.36	.001 and .040	.299/.009/.014

Note. sBAT FF and T_2^* are the dependent variables. Age and adiposity measurements are the main explanatory variables. In the multiple linear regressions, the set of additional explanatory variables is sex, age, and site. aVATvol and aSATvol are used both alone as single main explanatory variables and together (aVATvol and aSATvol) as two main explanatory variables. Beta = the unstandardized coefficient of the linear regressions. 95% CI = 95% confidence interval of Beta. R^2 = R^2 adjusted for the whole model. *P* values for the explanatory variables are two-tailed.

Abbreviations: aSATvol, volume of abdominal subcutaneous adipose tissue; aVATvol, volume of abdominal visceral adipose tissue; FF, fat fraction; NA, not applicable; sBAT, cervical-supraclavicular adipose tissue; sBMI, standardized body mass index; WHtR, waist-to-height ratio.

HOMA-IR (or $\log_{10}$HOMA-IR) were positive, whereas the associations with Matsuda index and DI_O were negative. For both sBAT FF and T_2^*, the strongest correlation was observed with Matsuda index.

When adjusting for sex, age, site, and whole-body adiposity, by means of sBMI, the relationship between sBAT FF and each of 2h glucose, Matsuda index, and HOMA-IR remained statistically significant (Table 4). However, the association between sBAT FF and DI_O and between sBAT T_2^* and the different glucose metabolism measurements did not remain significant.

When adjusting for sex, age, site, and local distribution of adiposity, by means of aVATvol and aSATvol, the glucose metabolism associations that remained significant were those between sBAT FF and each of 2h glucose and Matsuda index (Table 4). Further, 2h glucose but not Matsuda index remained significant when the models were additionally adjusted for bSAT FF (R^2 = .66, *P* = .020 for 2h glucose and R^2 = .64, *P* = .225 for Matsuda index, data not presented).

4 | DISCUSSION

In the present study, sBAT FF, but not sBAT T_2^*, was observed to correlate significantly with 2h glucose both before and after adjustment for sex, age, site, and adiposity. Considering sBAT FF as an MRI estimate of BAT and 2h glucose (inversely related to glucose tolerance) as an important diagnostic and research tool for diabetes, this result indicates a direct link between BAT and glucose metabolism, which is not confounded by the burden of adiposity. The maintained significant association after additional adjustment for bSAT FF, and implicitly WAT FF, strengthens this conclusion. The association between sBAT FF and 2h glucose is a novel observation in adolescents and a valuable contribution to BAT research aiming for prevention of obesity and metabolic diseases.

In the present study, no sex-related differences in either sBAT FF or T_2^* could be observed from group analyses, which is in line with previous FDG-PET/CT studies in pediatric patients targeting metabolically active BAT at room temperature.[4,19] A positive correlation between sBAT FF and age was observed, but as the correlation was very weak and model-dependent, the finding might be insignificant, obscured by the relatively narrow age span (10-20 years) or a result of an increasing overweight with age in the present cohort. The stronger but still weak positive correlation between sBAT T_2^* and age, persisting after inclusion of sex, adiposity, and glucose metabolism parameters as explanatory variables, indicates a decreased BAT content in the cervical-supraclavicular depot with increasing age.

TABLE 4 Associations of sBAT FF and T_2^* with measurements of glucose metabolism (main explanatory variables) obtained using simple linear regression and after adjustment for multiple factors using multiple linear regression

	Simple linear regression				Multiple linear regression					
Variables	**Beta**	**95% CI**	**R^2**	***P* value**	**Beta**	**95% CI**	**R^2**	***P* values**		
sBAT FF vs								**Main**	**Sex/Age/Site**	**sBMI**
2h glucose	1.38	0.80 to 1.96	.13	<.001	1.12	0.62 to 1.62	.54	<.001	.813/.006/.783	<.001
Matsuda index	−1.09	−1.36 to −0.82	.34	<.001	−0.52	−0.80 to −0.24	.53	<.001	.788/.061/.034	<.001
log_{10}HOMA-IR	10.90	8.11 to 13.69	.31	<.001	4.78	1.89 to 7.68	.52	.001	.675/.013/.087	<.001
DI_O	−0.54	−0.92 to −0.17	.05	.005	−0.18	−0.47 to 0.11	.49	.230	.796/.024/.053	<.001
sBAT FF vs								**Main**	**Sex/Age/Site**	**aVATvol/aSATvol**
2h glucose					0.77	0.32 to 1.23	.63	.001	.033/.060/.827	<.001/<.001
Matsuda index					−0.27	−0.55 to −0.001	.61	.049	.094/.049/.154	<.001/<.001
log_{10}HOMA-IR					1.37	−1.46 to 4.20	.60	.339	.026/.061/.133	<.001/.001
DI_O					−0.01	−0.27 to 0.25	.60	.967	.031/.022/.149	<.001/<.001
sBAT T_2* vs								**Main**	**Sex/Age/Site**	**sBMI**
2h glucose	0.63	0.02 to 1.25	.02	.044	0.19	−0.41 to 0.79	.35	.532	.891/<.001/.015	<.001
Matsuda index	−0.61	−0.93 to −0.30	.10	<.001	−0.20	−0.53 to 0.12	.38	.215	.796/<.001/.002	<.001
HOMA-IR	0.52	0.12 to 0.93	.04	.011	0.005	−0.39 to 0.40	.34	.981	.934/<.001/.009	<.001
DI_O	−0.24	−0.62 to 0.15	.004	.223	−0.04	−0.37 to 0.28	.36	.805	.801/<.001/.003	<.001
sBAT T_2* vs								**Main**	**Sex/Age/Site**	**aVATvol/aSATvol**
2h glucose					−0.01	−0.62 to 0.60	.36	.980	.317/.012/.022	.005/.021
Matsuda index					−0.10	−0.45 to 0.25	.38	.581	.284/.003/.010	.020/.043
HOMA-IR					−0.23	−0.65 to 0.20	.35	.288	.405/.019/.017	.003/.033
DI_O					0.06	−0.27 to 0.39	.37	.724	.225/.006/.014	.002/.067

Note. sBAT FF and T_2^* are the dependent variables. Glucose metabolism parameters are the main explanatory variables. In the multiple linear regressions, the two sets of additional explanatory variables are sex, age, site, and sBMI (Panels 1 and 3) and sex, age, site, aVATvol, and aSATvol (Panels 2 and 4). *Beta* = the unstandardized coefficient of the linear regressions. *95% CI* = 95% confidence interval of Beta. R^2 = R^2 adjusted for the whole model. *P* values for the explanatory variables are two-tailed. Units of glucose metabolism parameters: 2h glucose ($mmol \cdot l^{-1}$), Matsuda index ($dl \cdot mg^{-1} \cdot ml \cdot \mu U^{-1}$), HOMA-IR ($mmol \cdot l^{-1} \cdot \mu U \cdot ml^{-1}$), and DI_O ($l \cdot mmol^{-1}$).

Abbreviations: aSATvol, volume of abdominal subcutaneous adipose tissue; aVATvol, volume of abdominal visceral adipose tissue; DI_O, oral disposition index; FF, fat fraction; HOMA-IR, homeostatic model assessment of insulin resistance; sBAT, cervical-supraclavicular adipose tissue; sBMI, standardized body mass index

However, the association between T_2^* and age might have been confounded by image quality (discussed further ahead). In a previous MRI study, no detectable association between the MRI estimates of BAT and age was observed in children.[27] However, in a previous FDG-PET/CT study in pediatric patients, a higher prevalence of active BAT was obtained in pubertal compared with prepubertal subjects.[19] In the present study, the association of pubertal status was only evaluated together with sex, age, site, and sBMI using multiple regression analyses. As age proved to be a better explanatory variable in all analyses, pubertal status is not extensively discussed in this work.

Owing to a larger cohort and supplementary variables in the linear regressions, the present study reinforces previously observed associations between adiposity measurements and MRI estimates of BAT in subjects of similar age.[27,28] Both sBAT FF and T_2^* correlated positively with adiposity estimated with sBMI, WHtR, aVATvol, and aSATvol. All relationships remained significant after adjustment for sex, age, and site, indicating a lower BAT content in subjects with more severe obesity. According to R^2 from simple linear regression, sBAT FF and T_2^* showed stronger relationships to aVATvol than aSATvol. This has previously been indicated in adults[43] and might be a consequence of a similar lipid accumulation pattern in the sBAT and aVAT depots, both being internal and possibly more metabolically involved than the aSAT depot. The positive correlations of sBAT FF and T_2^* with whole-body adiposity (sBMI) agree with previous FDG-PET/CT studies performed on adults where inverse associations between adiposity and BAT activity have been observed.[11,12] Our results are also in line with observations in pediatric patients, for which individuals with visualized BAT activity showed less weight gain and smaller increases in aVATvol and aSATvol after successful treatment.[44] The significantly lower sBAT FF and T_2^* compared with bSAT FF and T_2^* agree with a previous study performed on subjects of similar age[27] and indicate a higher BAT amount in the sBAT depot.

Amongst the glucose metabolism parameters, sBAT FF correlated positively with 2h glucose and HOMA-IR, and negatively with Matsuda index, also after adjustment for sex, age, site, and whole-body adiposity by means of sBMI. Similar association patterns were observed for sBAT T_2^* but the correlations were weaker and did not persist after the supplementary adjustments. When adjusting for local distribution of adiposity (aVATvol and aSATvol), instead of whole-body adiposity, the relationship between sBAT FF, 2h glucose, and Matsuda index remained significant. After additionally adjusting for bSAT FF, only the association with 2h glucose persisted. This relationship was still significant after exclusion of two subjects with comparably small volumes of segmented bSAT and therefore possibly less reliable bSAT FF estimations. As 2h glucose is a clinical and research measurement for diagnosing diabetes, this result suggests a direct relationship between BAT and glucose metabolism. The non-significant associations with Matsuda index, HOMA-IR, and DI_O (derived from both plasma glucose and insulin levels) might be related to differences in measurement precision, a weaker relationship with insulin than with glucose or to 2h glucose being a superior parameter for reflecting impaired glucose metabolism.

Speculations regarding the underlying mechanisms to the association between sBAT and 2h glucose could include the capacity of BAT to dispose of blood glucose, possibly leading to improved glycaemic control,[31] and/or to its capacity to combust triglycerides and free fatty acids, potentially counteracting development of insulin resistance and obesity.[45] Other potential mechanisms could be effects of signalling molecules secreted from BAT, as suggested from BAT transplantation studies in rodents (discussed by Kiefer 2017[3]).

Overall, the results suggest a relationship between BAT and glucose metabolism, which is independent of the distribution of adiposity in the visceral and subcutaneous depots and thereby that BAT itself might have a role in the glucose metabolism of young subjects. This interpretation is in line with previous publications from related studies in adults, supporting a role for BAT in the glucose homeostasis and further suggesting it as a potential antidiabetic tissue.[30,31]

Compared with earlier publications on sBAT FF and T_2^* in children, the present study included more subjects (n = 143 compared with n = 39[27] and n = 28[28]), especially those with overweight and obesity, which enabled more reliable multiple regression analyses. However, a limitation is the small number of control subjects (17 individuals from Uppsala). The lack of Salzburg controls is not expected to have influenced the results considerably as the multiple linear regression models were adjusted for site. Although no statistically significant difference in the proportion of males and females between the groups was observed, the fractions should ideally have been more equal. From group comparisons between the Salzburg and Uppsala patients, differences with respect to several adiposity and glucose metabolism measurements were obtained. These results were likely due to the Uppsala patients being more affected by obesity and glucose intolerance as they were recruited at an obesity specialist clinic after referral from primary health care due to inadequate treatment results. In Salzburg, however, no referral was required and the subjects were therefore able to directly contact the clinic at which they were recruited. The lacking difference in 2h glucose between Salzburg patients and Uppsala controls could be due to a relatively unaltered glucose tolerance in the Salzburg patients or to a difference in the analysis procedure of the blood glucose samples, between Salzburg and Uppsala.

In this study, there were some limitations regarding the techniques used for data acquisition and analysis. The measurements of glucose metabolism were based on non-gold standard methods for insulin sensitivity and secretion. The gold standard methods are the hyperinsulinemic euglycaemic and hyperglycaemic clamp techniques, which have disadvantages such as being more invasive and complex, and as such more difficult to perform. Before the MRI, instructions on shallow breathing were provided to the subjects. The number of subjects excluded from the analyses (n = 18), primarily due to motion artefacts, reflects the difficulty in complying with these instructions. Older subjects likely performed better as their overall image quality tended to be superior. There is currently no non-invasive and non-ionizing reference technique for estimating BAT amount and activity. The MRI technique used in the present study is not BAT-specific but assumes BAT amount to be negatively correlated with sBAT FF and T_2^*. This assumption is based on differences in triglyceride, water, and iron content between BAT and WAT. However, as the proportion of brown adipocytes in sBAT varies amongst individuals,[8,9] and as these cells might undergo obesity-related whitening (similar to that observed in mice[46]), BAT detection using water-fat MRI is challenging. Although FF and T_2^* are relatively well-established MRI estimates of human BAT,[22-24] recent studies report a lack of relationships between BAT activity and the supraclavicular depot FF and T_2^*.[47,48] The inconsistent results between these two studies and others[24,26] might be because of differences and limitations in the quantification methods, eg, the use of the standardized uptake value instead of the more appropriate glucose uptake rate when studying obese subjects.[49] Because of the mixed content of sBAT, other measures that better reflect the relative number of brown adipocytes to white adipocytes, than the absolute value of FF, might be even more representative of BAT amount. For example, the difference in FF between SAT and supraclavicular fat in adults has shown a negative association with obesity and metabolic dysfunction.[45] Nevertheless, dedicated comparisons between different MRI estimates of BAT have not yet been performed and the most appropriate measures remain to be determined. In the present study, the confounding effects from WAT and general adiposity, to the glucose metabolism associations, were minimized by adjustments for sBMI, aVATvol, aSATvol, and bSAT FF.

The more prominent association between 2h glucose and sBAT FF, compared with T_2^*, could be due to either FF being a more suitable biomarker for BAT or to methodological limitations in the estimation of T_2^*. In this study, the MRI sBAT pulse sequence was optimized for quantification of FF, but not T_2^*, and the water-fat MR signal model was based on a joint T_2^* relaxation time for the water and fat signals. In addition, T_2^* is sensitive to magnetic field inhomogeneities and therefore dependent on the shimming performance, which is challenging in the shoulder

region. These limitations might contribute to the lacking relationships between T_2^* and the glucose metabolism parameters.

Future investigations of the underlying mechanisms to the association between BAT and 2h glucose in adolescents are warranted. Also, changes in sBAT FF and T_2^* before and after intervention, eg, bariatric surgery as recently studied,[50] are potential topics for forthcoming studies.

In conclusion, the association between sBAT FF and 2h glucose indicates a role for BAT in glucose metabolism, which potentially could influence the risk of developing diabetes. The lacking association with sBAT T_2^* might be due to FF being a superior biomarker for BAT and/or to methodological limitations in the quantification of T_2^*.

ACKNOWLEDGEMENTS

The research leading to these results has received funding from the European Union's Seventh Framework Programme (FP7/2007-2013) under grant agreement number 279153 (Beta-JUDO), the Swedish Research Council under grant agreement number 2016-01040, the Swedish Heart-Lung Foundation under grant agreement number 2170492, and the Regional Research Council in Uppsala, Sweden, under grant agreement number 309901 and 233041. We gratefully acknowledge the willingness of the Beta-JUDO volunteers and their families to participate in the study. We also thank Torgny Karlsson, Department of Immunology, Genetics and Pathology, Uppsala University, for advice on statistical analysis.

CONFLICTS OF INTEREST

D.W. has received consultant fees from Novo Nordisk. J.K. and H.A. are cofounders of Antaros Medical, where they are also partially employed. The remaining authors declare no conflicts of interest.

AUTHOR CONTRIBUTIONS

E.L., J.L., R.S., A.F., P.B., H.A., and J.K. participated in the particular study design. A.F., P.B., D.W., K.P., F.Z., K.W., M.M., H.A., and J.K. lead the full study which collected the data. E.L., J.A., R.S., and J.K. developed the methods and software for image analysis. E.L., J.A., and H. M. participated in data acquisition. J.L. performed the statistical evaluations. E.L. and J.L. wrote the main manuscript text. All critically reviewed and approved the final manuscript.

ORCID

Elin Lundström https://orcid.org/0000-0003-2955-4958
Joy Ljungberg https://orcid.org/0000-0002-6209-591X
Jonathan Andersson https://orcid.org/0000-0001-6477-2331
Hannes Manell https://orcid.org/0000-0002-5209-4841
Robin Strand https://orcid.org/0000-0001-7764-1787
Anders Forslund https://orcid.org/0000-0001-9109-4556
Peter Bergsten https://orcid.org/0000-0002-4937-8464
Daniel Weghuber https://orcid.org/0000-0002-4389-0379
Kurt Widhalm https://orcid.org/0000-0001-8700-5573
Matthias Meissnitzer https://orcid.org/0000-0003-2422-8838
Håkan Ahlström https://orcid.org/0000-0002-8701-969X
Joel Kullberg https://orcid.org/0000-0001-8205-7569

REFERENCES

1. Cypess AM, Kahn CR. Brown fat as a therapy for obesity and diabetes. *Curr Opin Endocrinol Diabetes Obes*. 2010;17(2):143-149.
2. Betz MJ, Enerbäck S. Human brown adipose tissue: what we have learned so far. *Diabetes*. 2015;64(7):2352-2360.
3. Kiefer FW. The significance of beige and brown fat in humans. *Endocr Connect*. 2017;6(5):R70-R79.
4. Drubach LA, Palmer EL 3rd, Connolly LP, Baker A, Zurakowski D, Cypess AM. Pediatric brown adipose tissue: detection, epidemiology, and differences from adults. *J Pediatr*. 2011;159(6):939-944.
5. Wu J, Boström P, Sparks LM, et al. Beige adipocytes are a distinct type of thermogenic fat cell in mouse and human. *Cell*. 2012;150(2):366-376.
6. Cypess AM, White AP, Vernochet C, et al. Anatomical localization, gene expression profiling and functional characterization of adult human neck brown fat. *Nat Med*. 2013;19(5):635-639.
7. Jespersen NZ, Larsen TJ, Peijs L, et al. A classical brown adipose tissue mRNA signature partly overlaps with brite in the supraclavicular region of adult humans. *Cell Metab*. 2013;17(5):798-805.
8. Zingaretti MC, Crosta F, Vitali A, et al. The presence of UCP1 demonstrates that metabolically active adipose tissue in the neck of adult humans truly represents brown adipose tissue. *FASEB J*. 2009;23(9):3113-3120.
9. Lee P, Zhao JT, Swarbrick MM, et al. High prevalence of brown adipose tissue in adult humans. *J Clin Endocrinol Metab*. 2011;96(8):2450-2455.
10. Wu J, Cohen P, Spiegelman BM. Adaptive thermogenesis in adipocytes: is beige the new brown? *Genes Dev*. 2013;27(3):234-250.
11. van Marken Lichtenbelt WD, Vanhommerig JW, Smulders NM, et al. Cold-activated brown adipose tissue in healthy men. *N Engl J Med*. 2009;360(15):1500-1508.
12. Vijgen GH, Bouvy ND, Teule GJ, Brans B, Schrauwen P, van Marken Lichtenbelt WD. Brown adipose tissue in morbidly obese subjects. *PLoS ONE*. 2011;6(2):e17247.
13. Cypess AM, Lehman S, Williams G, et al. Identification and importance of brown adipose tissue in adult humans. *N Engl J Med*. 2009;360(15):1509-1517.
14. Yoneshiro T, Aita S, Matsushita M, et al. Age-related decrease in cold-activated brown adipose tissue and accumulation of body fat in healthy humans. *Obesity (Silver Spring)*. 2011;19(9):1755-1760.
15. Au-Yong IT, Thorn N, Ganatra R, Perkins AC, Symonds ME. Brown adipose tissue and seasonal variation in humans. *Diabetes*. 2009;58(11):2583-2587.
16. Cypess AM, Chen YC, Sze C, et al. Cold but not sympathomimetics activates human brown adipose tissue in vivo. *Proc Natl Acad Sci U S A*. 2012;109(25):10001-10005.
17. van der Lans AA, Hoeks J, Brans B, et al. Cold acclimation recruits human brown fat and increases nonshivering thermogenesis. *J Clin Invest*. 2013;123(8):3395-3403.
18. van der Lans AA, Wierts R, Vosselman MJ, Schrauwen P, Brans B, van Marken Lichtenbelt WD. Cold-activated brown adipose tissue in human adults: methodological issues. *Am J Physiol Regul Integr Comp Physiol*. 2014;307(2):R103-R113.
19. Gilsanz V, Smith ML, Goodarzian F, Kim M, Wren TA, Hu HH. Changes in brown adipose tissue in boys and girls during childhood and puberty. *J Pediatr*. 2012;160(4):604-609 e601.

20. Simmonds M, Llewellyn A, Owen CG, Woolacott N. Predicting adult obesity from childhood obesity: a systematic review and meta-analysis. *Obes Rev*. 2016;17(2):95-107.
21. Berglund J, Kullberg J. Three-dimensional water/fat separation and T2* estimation based on whole-image optimization—application in breathhold liver imaging at 1.5 T. *Magn Reson Med*. 2012;67(6):1684-1693.
22. Hu HH, Perkins TG, Chia JM, Gilsanz V. Characterization of human brown adipose tissue by chemical-shift water-fat MRI. *AJR Am J Roentgenol*. 2013;200(1):177-183.
23. Gifford A, Towse TF, Walker RC, Avison MJ, Welch EB. Characterizing active and inactive brown adipose tissue in adult humans using PET-CT and MR imaging. *Am J Physiol Endocrinol Metab*. 2016;311(1):E95-E104.
24. Holstila M, Pesola M, Saari T, et al. MR signal-fat-fraction analysis and T2* weighted imaging measure BAT reliably on humans without cold exposure. *Metabolism*. 2017;70:23-30.
25. Chen KY, Cypess AM, Laughlin MR, et al. Brown adipose reporting criteria in imaging studies (BARCIST 1.0): recommendations for standardized FDG-PET/CT experiments in humans. *Cell Metab*. 2016;24(2):210-222.
26. Koskensalo K, Raiko J, Saari T, et al. Human brown adipose tissue temperature and fat fraction are related to its metabolic activity. *J Clin Endocrinol Metab*. 2017;102(4):1200-1207.
27. Hu HH, Yin L, Aggabao PC, Perkins TG, Chia JM, Gilsanz V. Comparison of brown and white adipose tissues in infants and children with chemical-shift-encoded water-fat MRI. *J Magn Reson Imaging*. 2013;38(4):885-896.
28. Deng J, Schoeneman SE, Zhang H, et al. MRI characterization of brown adipose tissue in obese and normal-weight children. *Pediatr Radiol*. 2015;45(11):1682-1689.
29. Orava J, Nuutila P, Lidell ME, et al. Different metabolic responses of human brown adipose tissue to activation by cold and insulin. *Cell Metab*. 2011;14(2):272-279.
30. Koksharova E, Ustyuzhanin D, Philippov Y, et al. The relationship between brown adipose tissue content in supraclavicular fat depots and insulin sensitivity in patients with type 2 diabetes mellitus and prediabetes. *Diabetes Technol Ther*. 2017;19(2):96-102.
31. Chondronikola M, Volpi E, Borsheim E, et al. Brown adipose tissue improves whole-body glucose homeostasis and insulin sensitivity in humans. *Diabetes*. 2014;63(12):4089-4099.
32. Hanssen MJ, Hoeks J, Brans B, et al. Short-term cold acclimation improves insulin sensitivity in patients with type 2 diabetes mellitus. *Nat Med*. 2015;21(8):863-865.
33. Forslund A, Staaf J, Kullberg J, Ciba I, Dahlbom M, Bergsten P. Uppsala longitudinal study of childhood obesity: protocol description. *Pediatrics*. 2014;133(2):e386-e393.
34. American Diabetes A. (2) Classification and diagnosis of diabetes. *Diabetes Care*. 2015;38(Suppl 1):S8-S16.
35. Matsuda M, DeFronzo RA. Insulin sensitivity indices obtained from oral glucose tolerance testing: comparison with the euglycemic insulin clamp. *Diabetes Care*. 1999;22(9):1462-1470.
36. Matthews DR, Hosker JP, Rudenski AS, Naylor BA, Treacher DF, Turner RC. Homeostasis model assessment: insulin resistance and beta-cell function from fasting plasma glucose and insulin concentrations in man. *Diabetologia*. 1985;28(7):412-419.
37. Utzschneider KM, Prigeon RL, Faulenbach MV, et al. Oral disposition index predicts the development of future diabetes above and beyond fasting and 2-h glucose levels. *Diabetes Care*. 2009;32(2):335-341.
38. Marshall WA, Tanner JM. Variations in pattern of pubertal changes in girls. *Arch Dis Child*. 1969;44(235):291-303.
39. Marshall WA, Tanner JM. Variations in the pattern of pubertal changes in boys. *Arch Dis Child*. 1970;45(239):13-23.
40. Berglund J, Johansson L, Ahlström H, Kullberg J. Three-point Dixon method enables whole-body water and fat imaging of obese subjects. *Magn Reson Med*. 2010;63(6):1659-1668.
41. Lundström E, Strand R, Forslund A, et al. Automated segmentation of human cervical-supraclavicular adipose tissue in magnetic resonance images. *Sci Rep*. 2017;7(1):3064.
42. Kullberg J, Hedström A, Brandberg J, et al. Automated analysis of liver fat, muscle and adipose tissue distribution from CT suitable for large-scale studies. *Sci Rep*. 2017;7(1):10425.
43. Franz D, Weidlich D, Freitag F, et al. Association of proton density fat fraction in adipose tissue with imaging-based and anthropometric obesity markers in adults. *Int J Obes (Lond)*. 2018;42(2):175-182.
44. Chalfant JS, Smith ML, Hu HH, et al. Inverse association between brown adipose tissue activation and white adipose tissue accumulation in successfully treated pediatric malignancy. *Am J Clin Nutr*. 2012;95(5):1144-1149.
45. Franssens BT, Hoogduin H, Leiner T, van der Graaf Y, Visseren FLJ. Relation between brown adipose tissue and measures of obesity and metabolic dysfunction in patients with cardiovascular disease. *J Magn Reson Imaging*. 2017;46(2):497-504.
46. Shimizu I, Aprahamian T, Kikuchi R, et al. Vascular rarefaction mediates whitening of brown fat in obesity. *J Clin Invest*. 2014;124(5):2099-2112.
47. McCallister A, Zhang L, Burant A, Katz L, Branca RT. A pilot study on the correlation between fat fraction values and glucose uptake values in supraclavicular fat by simultaneous PET/MRI. *Magn Reson Med*. 2017;78(5):1922-1932.
48. Deng J, Neff LM, Rubert NC, et al. MRI characterization of brown adipose tissue under thermal challenges in normal weight, overweight, and obese young men. *J Magn Reson Imaging*. 2018;47(4):936-947.
49. Borga M, Virtanen KA, Romu T, et al. Brown adipose tissue in humans: detection and functional analysis using PET (positron emission tomography), MRI (magnetic resonance imaging), and DECT (dual energy computed tomography). *Methods Enzymol*. 2014;537:141-159.
50. Hui SCN, Wong SKH, Ai Q, Yeung DKW, Ng EKW, Chu WCW. Observed changes in brown, white, hepatic and pancreatic fat after bariatric surgery: evaluation with MRI. *Eur Radiol*. 2018;29(2):849-856.

SUPPORTING INFORMATION

Additional supporting information may be found online in the Supporting Information section at the end of the article.

How to cite this article: Lundström E, Ljungberg J, Andersson J, et al. Brown adipose tissue estimated with the magnetic resonance imaging fat fraction is associated with glucose metabolism in adolescents. *Pediatric Obesity*. 2019;14:e12531. https://doi.org/10.1111/ijpo.12531